Published in final edited form as:
Biomacromolecules. 2012 June 11; 13(6): 1908–1915. doi:10.1021/bm300429e.

Synthesis and Characterization of Thermally and Chemically Gelling Injectable Hydrogels for Tissue Engineering

Adam K. Ekenseair, **Kristel W. M. Boere**, **Stephanie N. Tzouanas**, **Tiffany N. Vo**, **F. Kurtis Kasper**, and **Antonios G. Mikos***
Department of Bioengineering, Rice University, Houston, TX, 77030, USA

Abstract

Novel, injectable hydrogels were developed that solidify through a dual-gelation, physical and chemical, mechanism upon preparation and elevation of temperature to 37°C. A thermogelling, poly(N-isopropylacrylamide)-based macromer with pendant epoxy rings and a hydrolytically-degradable polyamidoamine-based diamine crosslinker were synthesized, characterized, and combined to produce *in situ* forming hydrogel constructs. Network formation through the epoxy-amine reaction was shown to be rapid and facile, and the progressive incorporation of the hydrophilic polyamidoamine crosslinker into the hydrogel was shown to mitigate the often problematic tendency of thermogelling materials to undergo significant post-formation gel syneresis. The results suggest that this novel class of injectable hydrogels may be attractive substrates for tissue engineering applications due to the synthetic versatility of the component materials and beneficial hydrogel gelation kinetics and stability.

Keywords

poly(N-isopropylacrylamide); polyamidoamine; tissue engineering; injectable; hydrogel

Introduction

While the majority of effort in tissue engineering research has been focused on pre-formed implantable scaffolds, there are many applications that might be better served with injectable, *in situ* forming materials capable of co-delivering cells and growth factors to optimize tissue regeneration. Injectable hydrogel-forming solutions can be applied via minimally invasive approaches, have generally high water contents to promote diffusion of nutrients and cells, and can easily fill complex tissue defects or voids often found in applications such as craniofacial bone regeneration after trauma, tumor resection, or birth defects.[1, 2] Various materials approaches to designing injectable hydrogel constructs have been previously reviewed.[3, 4]

Thermogelling polymers, which pass through a lower critical solution temperature (LCST) upon injection into the body, are promising candidates as scaffold backbones and have been recently reviewed.[5] In particular, hydrogels based on poly(N-isopropylacrylamide) (pNiPAAm), have been shown to have versatile and facile application towards the design of *in situ* forming hydrogel formulations. Previous efforts have identified numerous means to alter and control the rate and nature of the thermally-induced coil-globule phase transition of pNiPAAm to allow for system optimization,[6–10] have demonstrated the ability to successfully deliver encapsulated cells *in vitro*,[11–13] and have tested for efficacy as

*Corresponding author. mikos@rice.edu (A.G. Mikos).

injectable biomaterials *in vivo*.[14, 15] However, one major challenge associated with using thermoresponsive materials for the design of injectable constructs concerns the tendency of such polymeric gels to undergo syneresis after initial formation.[6, 16] In order to explore efficient therapies that ensure complete filling of tissue defects and promote contact and the exchange of nutrients and cells with the surrounding native tissue, this limitation must be addressed.

Recent investigations have focused on the creation of dual-hardening injectable hydrogels, which combine thermoresponsive polymers with concomitant *in situ* crosslinking to stabilize and strengthen the constructs.[6, 16–20] While some have utilized click chemistries to this end,[16, 21] many investigations have created crosslinking capacity in pNiPAAm hydrogels through polymer pendant-group modification to introduce reactive double bonds.[6, 17, 22] However, such systems require generally cytotoxic initiators and/or catalysts to be included in the injectable formulation to achieve crosslinking. Macromers of pNiPAAm modified with acrylate and methacrylate groups have been shown to be cytotoxic as well,[11] thus necessitating a rapid completion of the crosslinking reaction, which is generally accomplished through inclusion of catalyst compounds and/or high initiator concentrations. Despite these cytotoxicity concerns, pNiPAAm-based dual-hardening hydrogels have had some success at maintaining the viability of encapsulated mesenchymal stem cells and promoting construct mineralization.[12] An additional concern here is the ability of such crosslinks to degrade on a physiologically relevant timescale, as ester bonds located proximal to a polymer backbone are quite slow to degrade.[12] Thus, additional measures must be taken to promote network degradation, such as synthesis of complex pendant groups[9, 15] or introduction of degradability into the pNiPAAm backbone.[23]

In contrast to the use of a single macromer to both physically and chemically gel *in situ*, two-macromer systems offer a number of advantages. Key hydrogel properties, including hydrophilicity/degree of syneresis and the extent of crosslinking can be altered at the hydrogel formulation stage, as opposed to the macromer synthesis stage, through combination of a thermogelling macromer and a hydrophilic crosslinking macromer. By utilizing cytocompatible and degradable crosslinkers, optimization of the degradation and thermoresponsive behavior of the hydrogels can be compartmentalized. This route of construct design also allows for simplified and cost-effective polymer synthesis and access to a wide range of crosslinking chemistries.[22, 24, 25] However, material choice is limited to water-soluble, injectable polymers, which precludes use of many commonly employed degradable polymers, such as α-hydroxy esters.

Polyamidoamines (PAMAMs) are an emerging class of water-soluble and degradable macromers, thus far used primarily in the design of dendritic polymers and gene transfection agents.[26, 27] They have reported biocompatibility[28, 29] and facile synthesis procedures.[26, 30] The nature of the polyaddition reaction used in PAMAM synthesis allows for the straightforward production of linear, difunctional macromers with either amine or acrylamide termini. In addition, the rate of macromer degradation can be modulated through appropriate selection of the diamine and bisacrylamide comonomers,[31, 32] and additional reactive pendant moieties, such as hydroxyl or carboxylic acid groups, or higher-functionality crosslinkers can be easily incorporated into the macromer design.[26, 27, 33]

The objective of this study was to develop and characterize a novel injectable, thermally responsive, chemically crosslinkable, and hydrolytically degradable hydrogel. To this end, a thermogelling macromer based on pNiPAAm and a degradable PAMAM crosslinker were synthesized, characterized, and combined to create dual-hardening, injectable hydrogels. We hypothesized that the increased hydrogel hydrophilicity due to increasing PAMAM incorporation into the polymer network would mitigate the often problematic tendency of

thermogelling materials to undergo significant syneresis after hydrogel formation. We further hypothesized that an epoxy-based crosslinking reaction would allow for rapid and facile incorporation of the PAMAM macromer into the polymer network during and after thermogellation.

Materials and Methods

Materials

N-isopropylacrylamide (NiPAAm), glycidyl methacrylate (GMA), 2,2'-azobis(2-methypropionitrile) (azobisisobutyronitirle, AIBN), N,N'-methylenebisacrylamide (MBA), piperazine (PiP), and 0.1N sodium hydroxide solution were purchased from Sigma-Aldrich (Sigma, St. Louis, MO) and used as received. The solvents; tetrahydrofuran (THF), dimethylformamide (DMF), diethyl ether, and acetone in analytical grade, and water, acetonitrile, chloroform, and methanol in HPLC-grade; were obtained from VWR (Radnor, PA) and used as received. Phosphate-buffered saline (PBS) solution was mixed from powder (pH 7.4, Gibco Life, Grand Island, NY), and ultrapure water was obtained from a Millipore Super-Q water system (Millipore, Billerica, MA).

Thermogelling macromer (TGM) synthesis

The thermogelling macromer p(NiPAAm-co-GMA) was synthesized by free radical polymerization (Scheme 1). Ten grams of the comonomers, NiPAAm and GMA at 92.5 and 7.5 mol%, respectively, were dissolved in 100 mL of DMF and polymerized at 65°C under nitrogen atmosphere. AIBN was added as a free radical initiator at 0.7 mol% of the total monomer content, and the reaction mixture was continuously stirred for 20 h. The product was concentrated by rotary evaporation, dissolved in THF, and twice precipitated in at least 10-times excess of cold diethyl ether to effectively remove the unreacted monomers and low molecular weight oligomers. The final filtrate was dried under vacuum at ambient temperature to yield a fine white powder. In addition, a similar procedure was followed to create a pNiPAAm homopolymer.

Polyamidoamine synthesis

The polyamidoamine (PAMAM) crosslinking macromers were synthesized by polyaddition of PiP with MBA (Scheme 2). 10.83 g of the comonomers were dissolved in 30 mL ultrapure water with a stoichiometric excess of PiP (r = [MBA]/[PiP] = 0.846), stirred continuously under nitrogen atmosphere at 30°C, and allowed to react for 48 h according to published procedures.[26, 30] The obtained viscous mixture was directly precipitated in 100 mL acetone, filtered, and dried under vacuum at ambient temperature to yield a fine powder.

Proton Nuclear Magnetic Resonance Spectroscopy (^{1}H NMR)

^{1}H NMR spectra were obtained using a 400 MHz spectrometer (Bruker, Switzerland). Sample materials were dissolved in D_2O (typical concentration: 20 mg/mL) that contained 0.75 wt% 3-(trimethylsilyl)propionic-2,2,3,3-d_4 acid, sodium salt (TSP) as internal shift reference (Sigma-Aldrich, St. Louis, MO). All post-acquisition data processing was performed with the MestRe-C NMR software package (Mestrelab Research S.L., Spain). The free induction decay (FID) was Fourier transformed, manually phased, referenced using the TSP signal, baseline corrected, and integrated.

Gel Permeation Chromatography (GPC)

Molecular weight distributions of the p(NIPAAm-co-GMA) and pNiPAAm polymers were determined by GPC. A GPC system consisting of an HPLC pump (Waters, model 510, Milford, MA), an autosampler/injector (Waters, model 717), and a differential refractometer

(Waters, model 410) equipped with a series of analytical columns (Styragel guard column 20 mm, 4.6 × 30 mm; Styragel HR3, 5 mm, 4.6 × 300 mm; Sytragel HR1 column, 5 mm, 4.6 × 300 mm (all Waters)) was used with degassed chloroform as the eluent at a flow rate of 0.3 mL/min. Samples were prepared in chloroform at a concentration of 25 mg/mL and filtered prior to analysis. Macromer number average molecular weight (M_n) and polydispersity index (PDI) were determined in triplicate relative to polystyrene standards.

MicroTOF Mass Spectroscopy

Molecular weight distributions of the synthesized PAMAM crosslinker were analyzed using time-of-flight mass spectroscopy with positive-mode electrospray ionization on a Bruker microTOF ESI spectrometer (Bruker Daltonics, Billerica, MA) equipped with a 1200 series HPLC (Agilent Technologies, Santa Clara, CA) to deliver the mobile phase (50:50 HPLC-grade water and methanol). During the PAMAM synthesis, 100 μL samples of the reaction mixture were collected at 30 min and 1, 2, 4, 12, 24, and 48 h, diluted with 550 μL of a 50:50 mixture of HPLC-grade water and acetonitrile with 0.1% formic acid added, and a 2 μL flow injection was delivered to the electrospray chamber. After data acquisition, all peaks (including degradation and secondary reaction products) were identified using microTOF Control software (Bruker), corrected for charge state (generally with H^+ or Na^+ and rarely K^+ ions), and quantified for calculation of M_n, M_w, and PDI.

Differential Scanning Calorimetry (DSC)

The LCSTs of the thermogelling macromers were determined by DSC. 14 μL of 10 wt% polymer in pH 7.4 PBS solutions were pipetted into aluminum volatile sample pans (TA Instruments, Newcastle, DE) and capped/crimped. Thermograms were recorded in triplicate on a TA Instruments DSC 2920 equipped with a refrigerated cooling system against an empty sealed pan as reference. In a typical run, the oven was equilibrated at either 5°C or −5°C for 10 min and then heated to 80°C at a heating rate of 5°C/min. The LCST was determined both as the onset and peak temperature of the endothermic peak in the thermogram using the Universal Analysis 2000 software provided with the DSC system. In addition, the progress of the hydrogel formation/crosslinking reaction was monitored by DSC. 14 μL of the hydrogel solution (10 wt% TGM and 7 wt% PAMAM in pH 7.4 PBS) was pipetted into an aluminum pan, capped/crimped, placed into the DSC and equilibrated at 37°C, and monitored until the completion of the reaction.

Rheological Characterization

A thermostatted, oscillating rheometer (Rheolyst AR1000, TA Instruments, New Castle, DE) equipped with a 6 cm steel cone (1 degree) with a gap size of 26 μm was used to evaluate the elastic response of the hydrogels. Injectable hydrogel formulations containing 7 and 10 wt% (w/v) of PAMAM and TGM, respectively, in pH 7.4 PBS were pipetted onto the rheometer, and the dynamic viscoelastic properties of the solutions, namely, the dynamic shear storage (G') and loss (G") moduli, complex viscosity ($|\eta^*|$), and loss angle (δ), were recorded using the TA Rheology Advantage software (TA Instruments) as the solution was either maintained at a temperature of 18°C for 4 h or maintained at 4°C for 10 minutes followed by rapid elevation to and maintenance at 37°C for 3 h.

Hydrogel Formation and Degradation

Individual solutions of the TGM and PAMAM macromers were prepared at twice the desired final solution concentrations, and 250 μL of each TGM and PAMAM solution combination were combined in a glass vial at 4°C and mixed gently for ~30 s. The injectable solutions were then immediately immersed in a 37°C water bath and allowed 24 h to reach

equilibrium. After equilibrium swelling analysis, degradation of the PAMAM networks at 37°C was evaluated in both pH 7.4 PBS and 0.1N sodium hydroxide solution.

Cell Culture

A rat fibroblast cell line (ATCC, CRL-1764) was cultured on T-75 flasks using Dulbecco's modified Eagle medium (DMEM; Gibco Life, Grand Island, NY) supplemented with 10% (v/v) fetal bovine serum (FBS; Cambrex BioScience, Walkersville, MD) and 1% (v/v) antibiotics containing penicillin, streptomycin and amphotericin (Gibco Life). Cells were cultured in a humidified incubator at 37°C and 5% CO_2. Cells of passage number 3 were used in this study.

Cytocompatibility of Hydrogel Leachables

The cytocompatibility of the chemically and thermally gelled hydrogels were evaluated by a leachables extraction test, according to established protocols.[11, 34] Hydrogel discs were formed by injecting 90 μL aliquots of a 4°C solution with 7 and 10 wt% PAMAM and TGM, respectively, in cell culture media (DMEM, supplemented with antibiotics) without the addition of serum into Teflon molds (6 mm in diameter and 3 mm in height) held at 37°C and given 24 h to equilibrate. Hydrogels were then immersed in an excess of cell culture media without serum at a surface area to fluid volume ratio of 3 cm^2/mL and incubated at 37°C for 24 h.[34] The resulting hydrogel leachables solution was collected, sterile filtered, and prepared in 1, 10, and 100x dilutions. Cultured cells were harvested at 80–90% confluency with a Trypsin/EDTA solution (2 mL/flask), resuspended at a density of 100,000 cells/mL, and seeded into 96-well tissue culture plates (100 μL cell suspension/well) for a seeding density of 10,000 cells/well. The plates were then incubated for 24–48 h before testing to achieve 80–90% confluency within the well. The three dilutions of extract media were added to the cultured fibroblast cells in the 96-well plates (100 μL/well), replacing the culture media (n = 6). In addition, cells fed with identical media without the extracted leachables (DMEM supplemented with antibiotics and without serum) served as a positive (live) control, and cells exposed to 70% ethanol for 10 min served as the negative (dead) control (n=6). The plates were then incubated at 37°C, 95% relative humidity, and 5% CO_2 for either 2 or 24 h.

Following incubation, media were removed, the cells were rinsed three times with pH 7.4 PBS, calcein AM and ethidium homodimer-1 in 2 μM and 4 μM concentrations in PBS, respectively (Live/Dead viability/cytotoxicity kit, Molecular Probes, Eugene, OR), were added, and the cells were incubated in the dark at room temperature for 30 min. Cell viability was then quantified using a fluorescence plate reader (Biotek Instrument FLx800, Winooski, VT) equipped with filter sets of 485/528 nm (excitation/emission) for calcein AM (live cells) and 528/620 nm (excitation/emission) for EthD-1 (dead cells). The fluorescence of the cell populations was recorded and the fractions of live and dead cells were calculated relative to the controls. The data are expressed as mean ± standard deviation, and statistically significant differences were determined by Tukey's post hoc test.

Results and Discussion

TGM Synthesis

Homopolymers of pNiPAAm and copolymers with GMA were successfully synthesized to yield thermoresponsive macromers with functional pendant epoxide moieties. The number average molecular weight, M_n, and polydispersity index (PDI) of the synthesized pNiPAAm macromer were 8.9 ± 0.1 kDa and 2.72 ± 0.08, respectively, as determined by GPC (data not shown). Similarly, values of M_n = 9.2 ± 0.6 kDa and PDI = 3.12 ± 0.04 were found for p(NiPAAm-co-GMA).

Copolymer composition was further evaluated by ^{1}H NMR. Figure 1 shows the ^{1}H NMR spectra of p(NiPAAm-co-GMA). The five individual pendant proton signals (3d and 2e) on GMA were found between 2.5 and 4.8 ppm, along with the isopropyl proton from NiPAAm (1a, 3.8–3.9). The six NiPAAm methyl protons (6b) were found from 0.9 – 1.3, and the polymer backbone protons (3c, 3f) were located from 1.3 – 2.3 ppm. The proton locations were confirmed by comparison with spectra of the NiPAAm and GMA monomers and the pNiPAAm homopolymer (data not shown). The varied peak locations allowed for five independent calculations of the GMA content in the copolymer through the relative intensities of the GMA and NiPAAm protons giving an average value of 7.44 ± 1.12 mol%, which compares well with the theoretical GMA content (7.5 mol%).

Finally, the LCSTs of the homopolymer and copolymer were determined by DSC (Figure 2). The onset and peak LCST for pNiPAAm were 29.5 ± 0.2°C and 33.3 ± 0.2°C, respectively, which compare well with the commonly reported LCST of 32°C. Copolymerization with GMA reduced the LCST to an onset of 22.2 ± 0.7°C and a peak of 30.9 ± 0.4°C. In addition, p(NiPAAm-co-GMA) displayed lower overall transition energy and a broader temperature distribution compared with the homopolymer, which can be attributed to lower overall NiPAAm content and greater chain content variation in the copolymer, respectively. The onset LCSTs as determined by DSC correlated very well to macroscopic observation of the temperatures at which thermogellation occurred (data not shown).

PAMAM Synthesis

An epoxy-reactive polyamidoamine diamine crosslinker was successfully synthesized by adapting reported protocols.[26, 30] Figure 3 shows the ^{1}H NMR spectrum of the final purified and dried product of the PAMAM synthesis. The expected molecular structure of the diamine product is shown with protons and their corresponding peak locations are identified. The peak locations were confirmed by analysis of the MBA and PiP comonomers (data not shown). A crude estimate of the number average degree of polymerization can be calculated based on functional group quantification and assuming 100% conversion of the limiting reactant (MBA) as shown in Figure 3. Application of these equations yielded r = 0.840 and X_n = 11.52 (M_n = 1350). These values compared favorably with the feed stoichiometric ratio (r = 0.846) and expected molecular weight (X_n = 11.99, M_n = 1400 D), assuming 100% conversion of MBA.

This molecular weight calculation assumed that all of the functional groups present were part of chains of the product diamine. However, since the product is susceptible to hydrolytic degradation and the synthesis was run in water, further analysis of the actual product compositions was necessary.[35] To this end, time-of-flight mass spectroscopy analysis with electrospray ionization (microTOF mass spectroscopy) was utilized to identify and quantify the distribution of chain species present. Figure 4 displays the resulting raw data of signal intensity versus absolute mass with major peaks and associated charge states identified. Charge states of peak families were determined through measurement of the separation of isomeric peaks, as shown in the insert.

MicroTOF mass spectroscopy led to the successful identification, based on expected degradation products and their subsequent potential reactions, of all major species present in the final PAMAM product, as summarized in Table 1. Each compound identified appeared at numerous molecular weights and varying charge states. In addition to proton charges, sodium and occasional potassium adducts were also observed. Thus, the peaks were deconvoluted, summed, and assigned structures with matching absolute molecular weight values: (a) is the desired diamine PAMAM product; (b) is the heteroend version of the desired product; (c) and (g) are simple degradation products; and the remainder are secondary products of the reaction of either the primary amine groups ((e) and (f)) or the

carboxylic acid groups ((d) and (h)) resulting from hydrolytic degradation of the PAMAM amide linkages.

It should also be mentioned that each product structure shown is the representative or simplest form of that particular product, with the degradation and secondary reaction products shown at the end of a PAMAM chain. However, further addition of repeat units is often possible beyond the end groups. Thus, each degradation and secondary reaction product shown represents a class of polymer species having the same molecular weight and functional end groups. Also shown in Table 1 are the mol percents of each species identified, as determined from the relative microTOF peak intensities, and a further product analysis is presented in Table 2.

The desired PAMAM diamine comprises 88.5 mol% and 95.2 wt% of the total reaction product, with the difference a result of the inherently smaller nature of species originating from degradation pathways. Including the side-products and degradation-derived products of the synthesis scheme utilized, 98.5 wt% of the resultant powder will participate in epoxy reactions with the TGM macromer, with 95.2 wt% having the potential to create crosslinks and 3.3 wt% simply the potential to form hydrophilic grafts. The remaining 1.5 wt% is comprised of species with non-amine functional ends, namely carboxylic and acrylamide functional ends (structures shown in Table 1). It should be mentioned, however, that the accuracy of such compositional quantifications could be limited by the nature of the mass spectroscopy analysis. Namely, we are assuming that all species are equally ionizable, evenly electrosprayed, and the detection signal is linear over more than two orders of magnitude.

Based on initial experimental observation, it was hypothesized that the polyamidoamine reaction likely was completed much earlier than the 48 h reaction time period, which was chosen based on published reports.[30] The hope was that optimizing the reaction timescale would result in fewer degradation and secondary reaction products. To this end, the reaction kinetics were investigated by sampling the reaction mixture over time and performing microTOF mass spectroscopy. The results of the transient reaction products study are summarized in Figure 5, where M_n and the total desired product diamine weight fraction (of the total species present in the reaction media) are shown over the course of the reaction (at 30 min, 1, 2, 4, 12, 24, and 48 h).

As hypothesized, the reaction primarily occurs and has nearly completed within the first 4 h, however no further change in the content of degradation and secondary reaction products was seen beyond the completion of the primary reaction. The absence of such a trend in retrospect can be attributed to the changing nature of the reaction media as functional groups are consumed. Namely, the rapid consumption of amine groups during the polyaddition reaction led to a significant decrease in the availability of base groups with associated decreases in the pH of the reaction solution (Figure 5 insert). Since the hydrolytic degradation is base catalyzed, the vast majority of degradation could be anticipated to occur in the very early stages of the synthesis procedure.

This hypothesis is borne out in preliminary PAMAM and hydrogel degradation studies, where the rate of degradation is more than an order of magnitude faster at pH 10 compared to pH 7.4. The ~2 kDa M_n (with a PDI of ~1.5) is higher than that found from ^{1}H NMR analysis and expected from theory, but represents only the desired diamine distribution. When all species were included in the calculation, the M_n was ~1.8 kDa. Finally, alternate solvents were investigated for the synthesis of the PAMAM diamine that might result in less product degradation, however due to component solubilities and the need for a protic solvent,[26] an alternative was not identified.

Hydrogel Formation

The TGM and PAMAM macromers were combined as synthesized in pH 7.4 PBS to create injectable, *in situ* dual-hardening solutions. Upon macromer mixing and increasing the temperature to 37°C, the solutions will rapidly solidify due to the thermogellation mechanism. Subsequently, the hydrogels will be stabilized and further hardened through epoxy-based chemical crosslinking to create a degradable polymer network structure (Figure 6).

Figure 7 illustrates the effect of progressive incorporation of the PAMAM crosslinker into 10 wt% TGM injectable solutions, with the equilibrium volume swelling ratio relative to the 0 wt% PAMAM hydrogel, Q_r, shown. As hypothesized, the increased hydrogel hydrophilicity mitigated the often problematic tendency of thermogelling solutions to undergo significant post-formation syneresis, while maintaining the ability of the TGM to undergo thermogellation at 37°C. It should also be noted that the theoretical maximum degree of crosslinking for this particular combination of TGM and PAMAM macromers is ~7 wt% PAMAM for 10 wt% TGM, as determined from quantification of reactive amine and epoxy functionalities per unit mass for each macromer. Thus, beyond 7 wt% PAMAM, the fraction of PAMAM molecules forming intermolecular crosslinks or intramolecular loops will decrease as some are replaced by hydrophilic branches.

The kinetics of the epoxy crosslinking reaction were first monitored thermally by DSC for injectable hydrogel solutions with 10 and 7 wt% of TGM and PAMAM, respectively. As can be seen in Figure 8, the crosslinking reaction was completed within 110 minutes. Such rapid *in situ* hardening of the thermogelled hydrogel constructs enhances gel stability while minimizing exposure of encapsulated cells and surrounding tissue to reactive species. Further evidence of the progress of the crosslinking reaction was seen in rheology traces. Figure 9 shows the rheological response of the hydrogels to crosslinking both in the presence (4/37°C) and absence (18°C) of physical thermogellation. Thus, the dual, thermally and physically, gelling nature of the hydrogel system is clearly illustrated.

Network formation in the absence of thermogellation at 18°C resulted in hydrogels that reached the gel point in ~100 min and had ultimate shear storage moduli, G', on the order of 1 kPa. Network formation in the presence of thermogellation at 37°C reached the gel point at ~60 min and showed the relative contributions of the physical and thermal gelation mechanisms, with an ultimate shear storage modulus, G', on the order of 90 kPa. The timescale of the crosslinking reaction as shown by rheology was somewhat lengthier than that shown by DSC (~180 and ~110 min, respectively). This is likely a reflection of rapid initial reaction followed by slower reaction of the incorporated but unreacted (dangling) amine functionalities, with associated network rearrangement, after the onset of the chemical gelation. The even longer timescales of chemical gelation and completion of crosslinking at 18°C was simply a reflection of lower rates of reaction and diffusion at the lower temperature.

After equilibrium swelling analysis, hydrogels were allowed to degrade at 37°C in pH 7.4 PBS. Figure 10 shows the rapid mass loss of the hydrogels associated with the degradation of the PAMAM crosslinkers beginning at seven and terminating at ten weeks. While this is likely to be an appropriate degradation timescale for many tissue engineering applications, it is worth pointing out once more that one of the major advantages of this novel class of polyamidoamine-based injectable hydrogels is the documented ability to easily tune the rate of polymer degradation as needed through alteration of the PAMAM backbone.[31, 32] Additionally, the hydrogels were evaluated under base-catalyzed accelerated degradation conditions, whereby 1 mL of 0.1N sodium hydroxide solution was added to each vial in

place of PBS. Within 4 days, hydrolytic degradation of the PAMAM crosslinkers was completed in all gels to yield clear liquid solutions at 4°C (data not shown).

Finally, initial cytocompatibility of the hydrogels was evaluated through exposure of rat fibroblasts to the soluble hydrogel leachables with fluorescent Live/Dead analysis after 2 and 24 h. Figure 11 shows the resulting fraction of live cells treated with 1, 10 and 100x dilutions of the hydrogel leachables in media relative to the untreated live control. The hydrogels were shown to be fully cytocompatible at all conditions tested, which was largely expected from the wealth of literature showing the general cytocompatibility of PNiPAAm-based and polyamidoamine-based macromers, as discussed in the introduction.

Conclusions

A novel injectable dual-hardening hydrogel was developed through synthesis and combination of a pNiPAAm-based thermogelling macromer and a hydrophilic and degradable polyamidoamine crosslinking macromer. Network formation through the epoxy crosslinking reaction was shown to be rapid and facile, with the reaction reaching completion in less than three hours after an initial thermogellation time of 2–3 seconds. Additionally, the often problematic tendency of thermogelling systems to undergo significant post-formation gel syneresis was mitigated through the combination of increased hydrogel hydrophilicity and gel hardening through concomitant chemical crosslinking during and after initial thermogellation.

Such *in situ* dual-hardening, dimensionally stable, defect-filling, and degradable hydrogels with high gel water content are attractive substrates for tissue engineering and cellular delivery applications. In particular, the use of water-soluble and degradable polyamidoamine polyaddition-formed macromers offers tremendous synthetic flexibility and control over subsequent gel properties. With the ability to tune hydrogel hydrophilicity, degree of post-formation swelling or syneresis, degradation timescale, degree of crosslinking, and potential introduction of additional pendant functional moieties with appropriate selection of starting comonomers, this study introduces a promising and versatile family of injectable *in situ* forming hydrogels that merit additional investigation.

Acknowledgments

This work was supported by a grant from the National Institutes of Health (R01 DE17441) and Baylor's Scientific Training Program for Dental Academic Research (T32 DE018380).

References

1. Gutowska A, Jeong B, Jasionowski M. Anat. Rec. 2001; 263:342–349. [PubMed: 11500810]
2. Temenoff JS, Mikos AG. Biomaterials. 2000; 21:2405–2412. [PubMed: 11055288]
3. Kretlow JD, Klouda L, Mikos AG. Adv. Drug Delivery Rev. 2007; 59:263–273.
4. Kretlow JD, Young S, Klouda L, Wong M, Mikos AG. Adv. Mater. 2009; 21:3368–3393. [PubMed: 19750143]
5. Klouda L, Mikos AG. Eur. J. Pharm. Biopharm. 2008; 68:34–45. [PubMed: 17881200]
6. Hacker MC, Klouda L, Ma BB, Kretlow JD, Mikos AG. Biomacromolecules. 2008; 9:1558–1570. [PubMed: 18481893]
7. Emik S, Gurdag G. J. Appl. Polym. Sci. 2006; 100:428–438.
8. Guan JJ, Hong Y, Ma ZW, Wagner WR. Biomacromolecules. 2008; 9:1283–1292. [PubMed: 18324775]
9. Ma ZW, Nelson DM, Hong Y, Wagner WR. Biomacromolecules. 2010; 11:1873–1881. [PubMed: 20575552]

10. Cui ZW, Lee BH, Pauken C, Vernon BL. J. Biomater. Sci. Polym. Ed. 2010; 21:913–926. [PubMed: 20482992]
11. Klouda L, Hacker MC, Kretlow JD, Mikos AG. Biomaterials. 2009; 30:4558–4566. [PubMed: 19515420]
12. Klouda L, Perkins KR, Watson BM, Hacker MC, Bryant SJ, Raphael RM, Kasper FK, Mikos AG. Acta Biomater. 2011; 7:1460–1467. [PubMed: 21187170]
13. Li ZQ, Guo XL, Matsushita S, Guan JJ. Biomaterials. 2011; 32:3220–3232. [PubMed: 21296413]
14. Cui ZW, Lee BH, Pauken C, Vernon BL. J. Biomed. Mater. Res. Part A. 2011; 98A:159–166.
15. Fujimoto KL, Ma ZW, Nelson DM, Hashizume R, Guan JJ, Tobita K, Wagner WR. Biomaterials. 2009; 30:4357–4368. [PubMed: 19487021]
16. Robb SA, Lee BH, McLemore R, Vernon BL. Biomacromolecules. 2007; 8:2294–2300. [PubMed: 17567067]
17. Kretlow JD, Hacker MC, Klouda L, Ma BB, Mikos AG. Biomacromolecules. 2010; 11:797–805. [PubMed: 20121076]
18. Cellesi F, Tirelli N, Hubbell JA. Macromol. Chem. Phys. 2002; 203:1466–1472.
19. Cellesi F, Tirelli N, Hubbell JA. Biomaterials. 2004; 25:5115–5124. [PubMed: 15109835]
20. Lee BH, West B, McLemore R, Pauken C, Vernon BL. Biomacromolecules. 2006; 7:2059–2064. [PubMed: 16768434]
21. Wang ZC, Xu XD, Chen CS, Yun L, Song JC, Zhang XZ, Zhuo RX. ACS Appl. Mater. Interfaces. 2010; 2:1009–1018. [PubMed: 20423120]
22. Cheng V, Lee BH, Pauken C, Vernon BL. J. Appl. Polym. Sci. 2007; 106:1201–1207.
23. Mizuntani M, Satoh K, Kamigaito M. Macromolecules. 2011; 44:2382–2386.
24. Wei HL, Yang Z, Chu HJ, Zhu J, Li ZC, Cui JS. Polymer. 2010; 51:1694–1702.
25. Wang ZC, Xu XD, Chen CS, Wang GR, Cheng SX, Zhang XZ, Zhuo RX. React. Funct. Polym. 2009; 69:14–19.
26. Ferruti P, Marchisio MA, Duncan R. Macromol. Rapid Commun. 2002; 23:332–355.
27. Lin C, Zhong ZY, Lok MC, Jiang XL, Hennink WE, Feijen J, Engbersen JFJ. Bioconjugate Chem. 2007; 18:138–145.
28. Magnaghi V, Conte V, Procacci P, Pivato G, Cortese P, Cavalli E, Pajardi G, Ranucci E, Fenili F, Manfredi A, Ferruti P. J. Biomed. Mater. Res. Part A. 2011; 98A:19–30.
29. Navath RS, Menjoge AR, Dai H, Romero R, Kannan S, Kannan RM. Mol. Pharm. 2011; 8:1209–1223. [PubMed: 21615144]
30. Dey RK, Ray AR. J. Macromol. Sci. Part A: Pure Appl. Chem. 2005; A42:351–364.
31. Jain R, Standley SM, Frechet JMJ. Macromolecules. 2007; 40:452–457.
32. Ferruti P, Ranucci E, Sartore L, Bignotti F, Marchisio MA, Bianciardi P, Veronese FM. Biomaterials. 1994; 15:1235–1241. [PubMed: 7703320]
33. Ferruti P, Manzoni S, Richardson SCW, Duncan R, Pattrick NG, Mendichi R, Casolaro M. Macromolecules. 2000; 33:7793–7800.
34. Timmer MD, Shin H, Horch RA, Ambrose CG, Mikos AG. Biomacromolecules. 2003; 4:1026–1033. [PubMed: 12857088]
35. Lynn DM, Langer R. J. Am. Chem. Soc. 2000; 122:10761–10768.

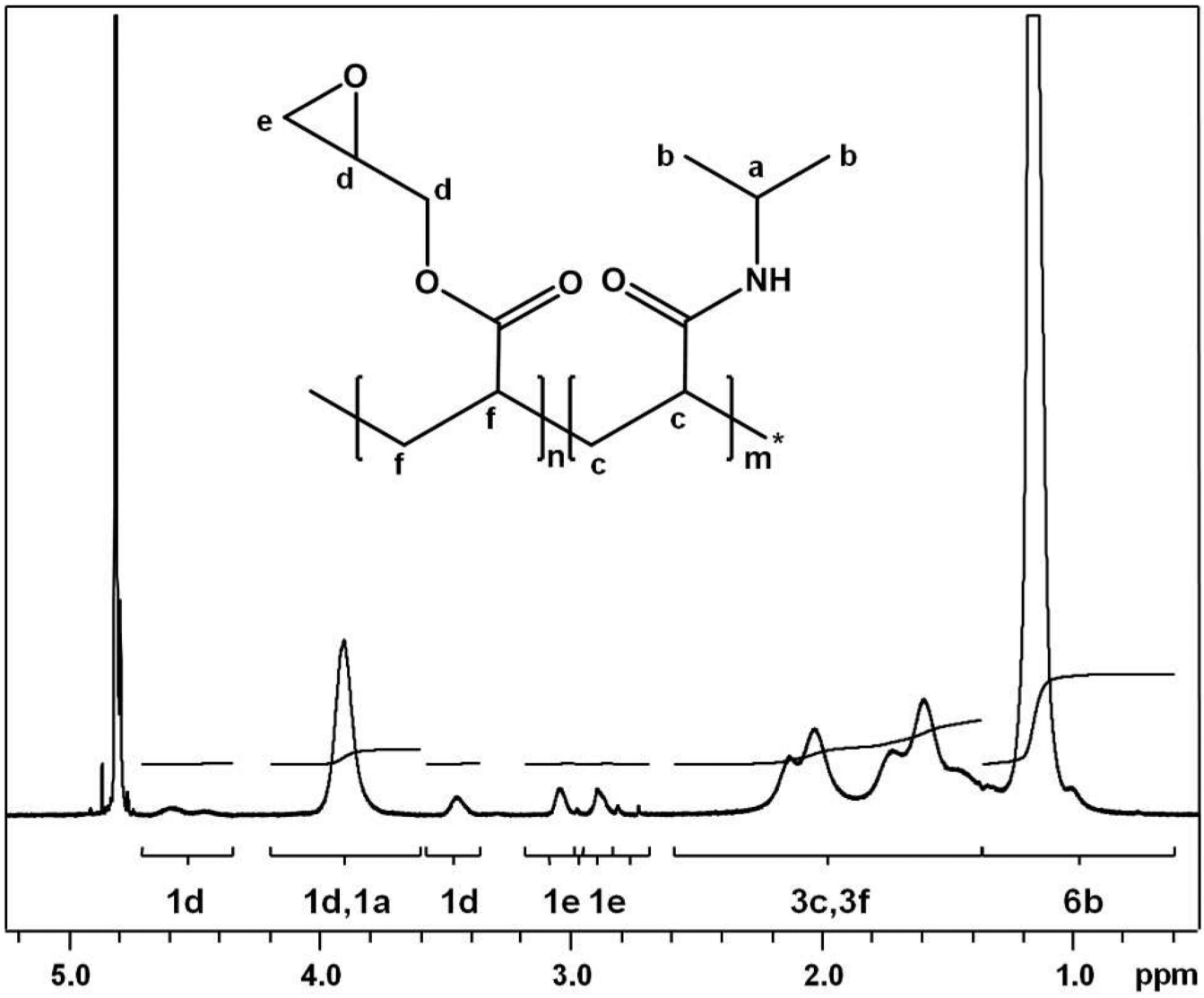

Figure 1.
^{1}H NMR spectra of p(NiPAAm-co-GMA) with proton peak locations identified.

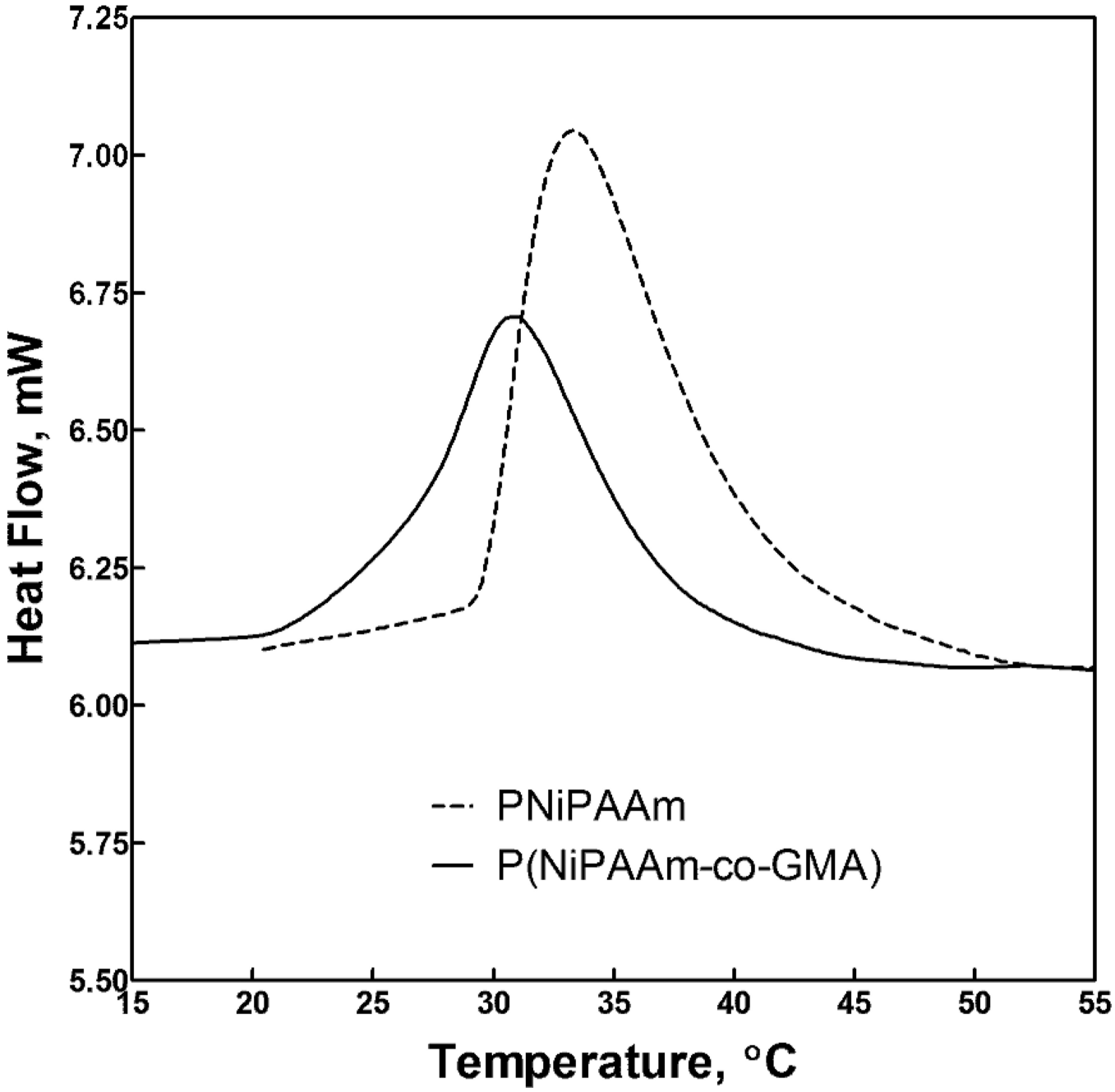

Figure 2.
DSC thermograms for pNiPAAm and p(NiPAAm-co-GMA) at 10 wt% polymer in pH 7.4 PBS solutions.

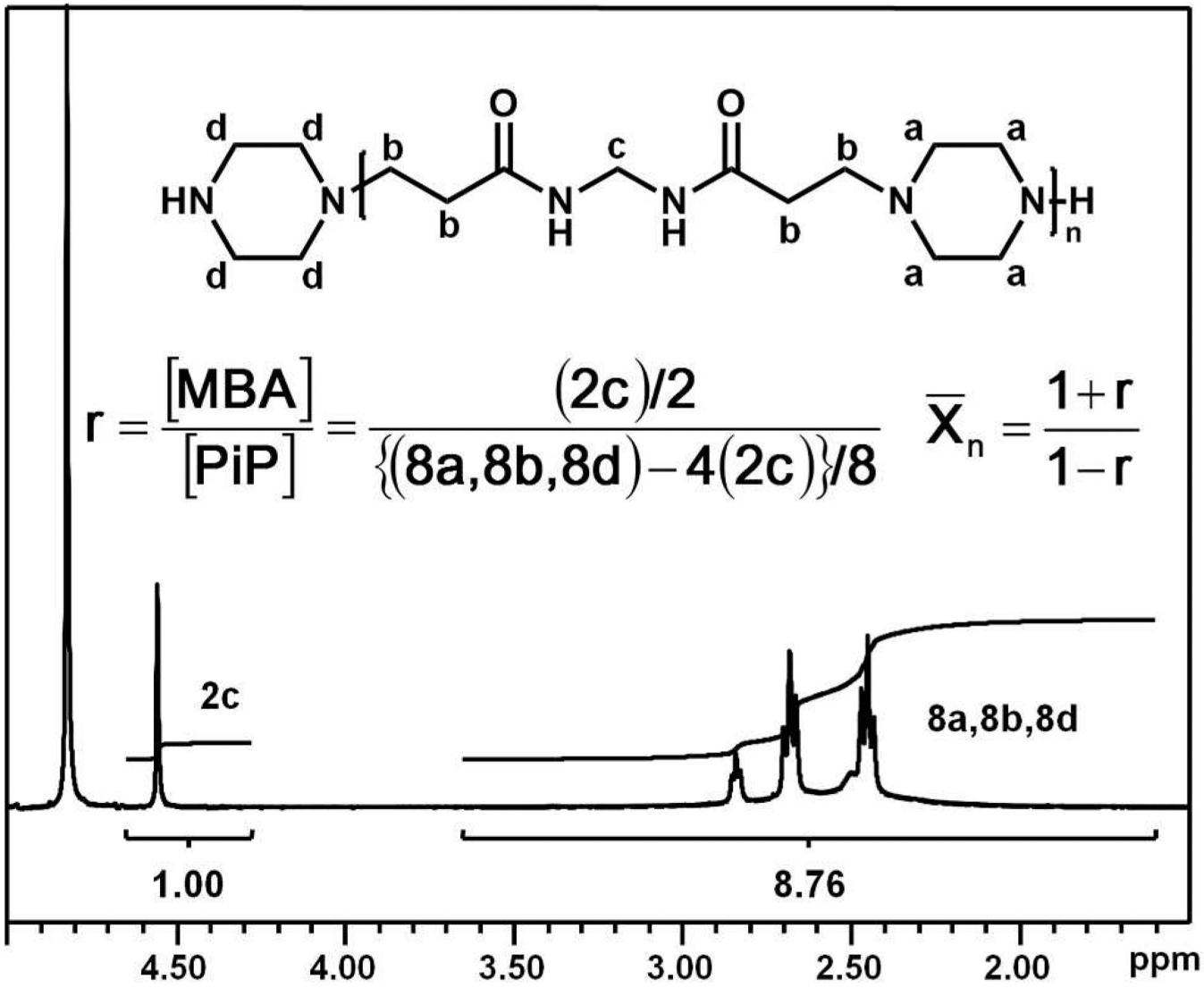

Figure 3.
^{1}H NMR spectra of PAMAM with proton peak locations identified and equations utilized to calculate an experimental average molecular weight based on peak intensities displayed.

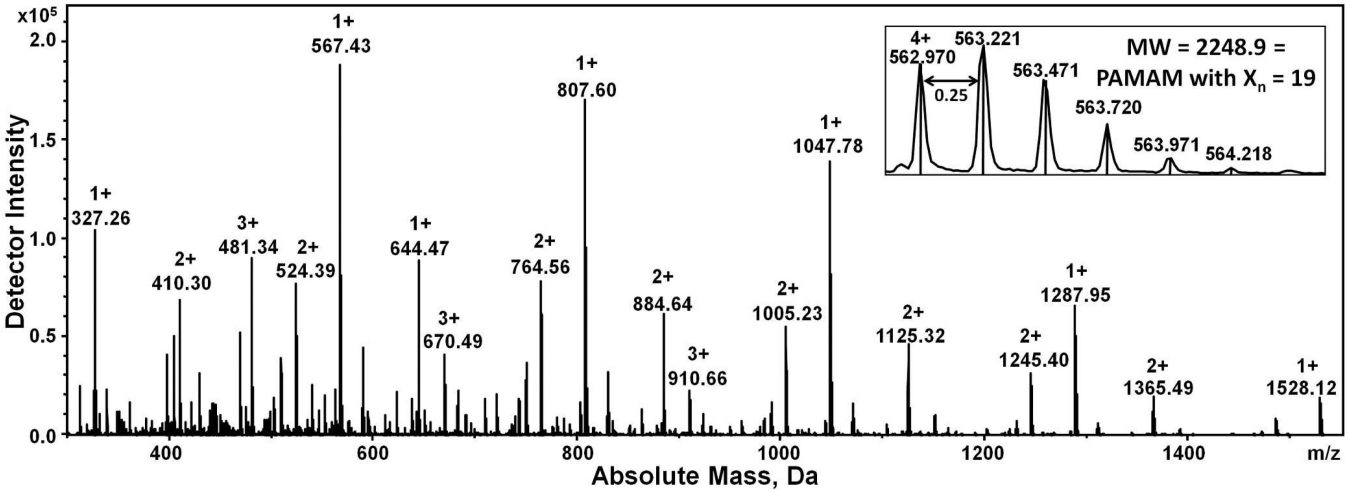

Figure 4.

Raw microTOF mass spectroscopy data for purified/dried PAMAM crosslinker showing molecular weights and charge states for some of the largest peaks, with a close-up view of a single peak family (insert).

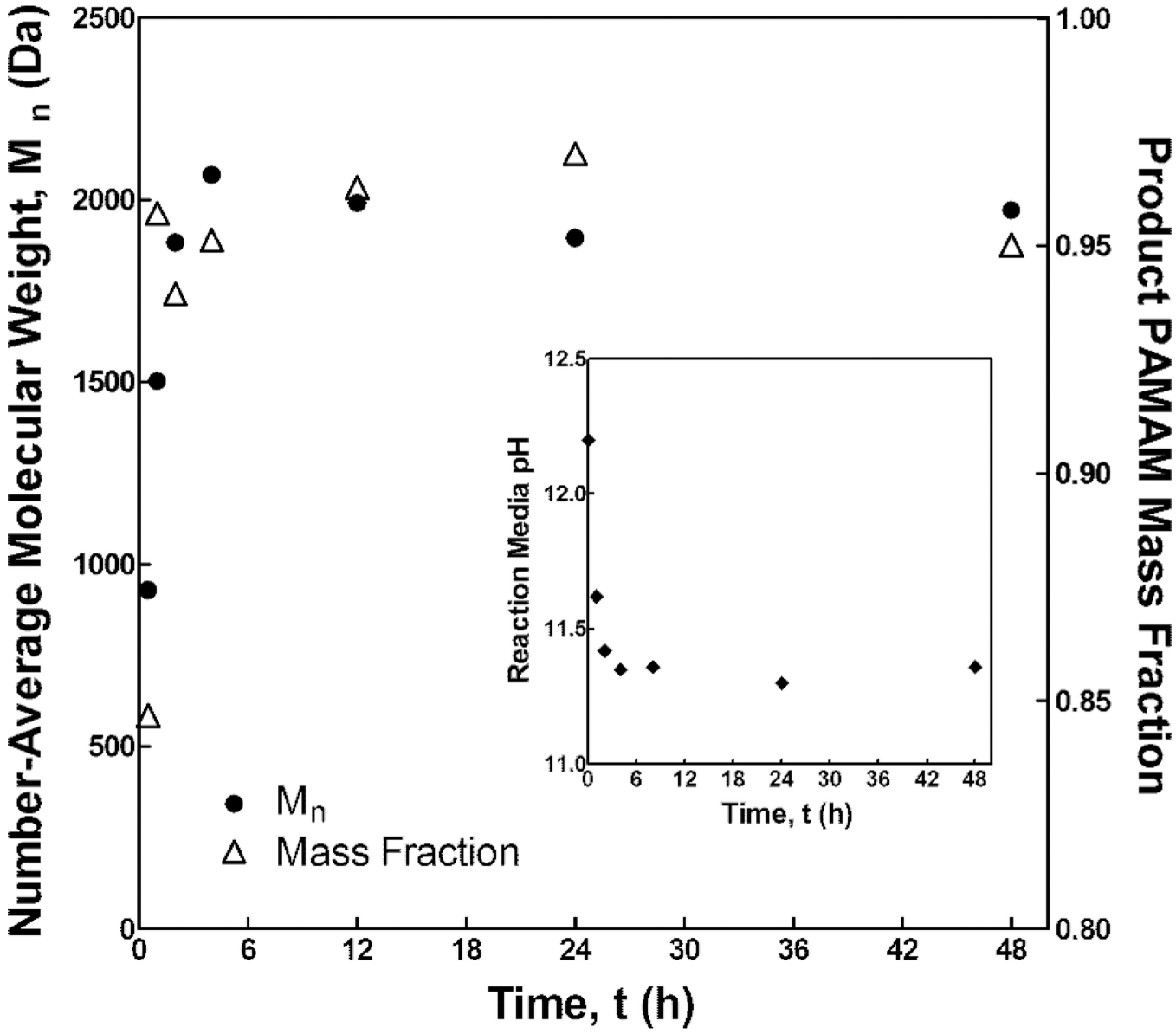

Figure 5.
Desired PAMAM diamine product M_n and weight fraction of the total reaction products, as determined by microTOF mass spectroscopy, and reaction media pH (insert) over the course of the synthesis reaction.

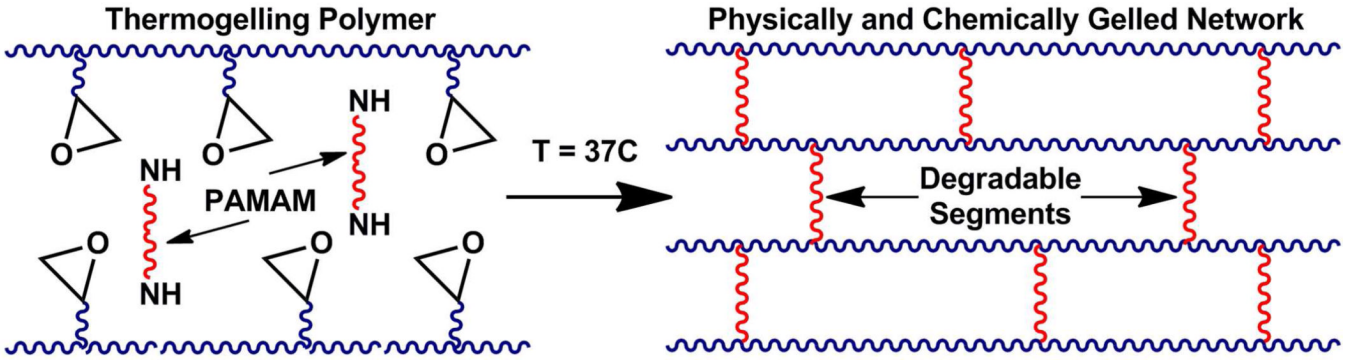

Figure 6.
Schematic representation of the hydrogel epoxy crosslinking reaction.

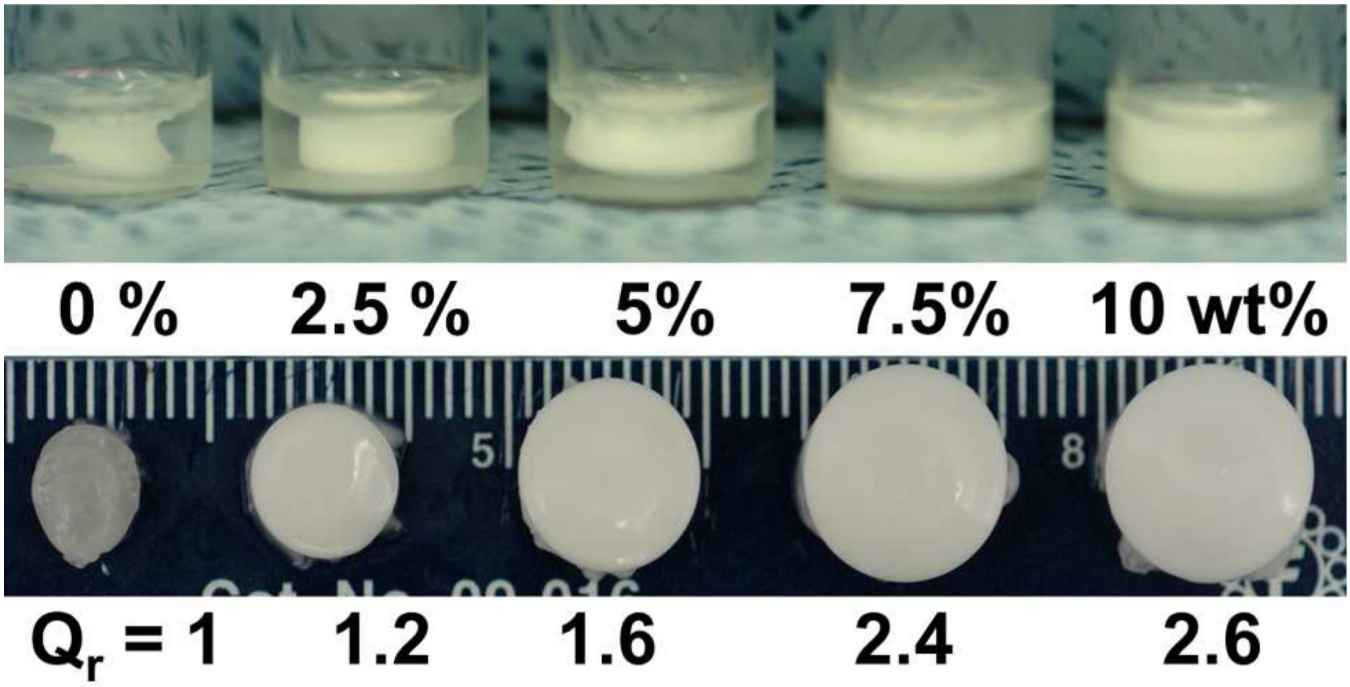

Figure 7.
Hydrogel formation and syneresis with 10 wt% TGM and varying PAMAM content (0 – 10 wt%) with volume swelling ratio relative to 0% PAMAM, Q_r, shown.

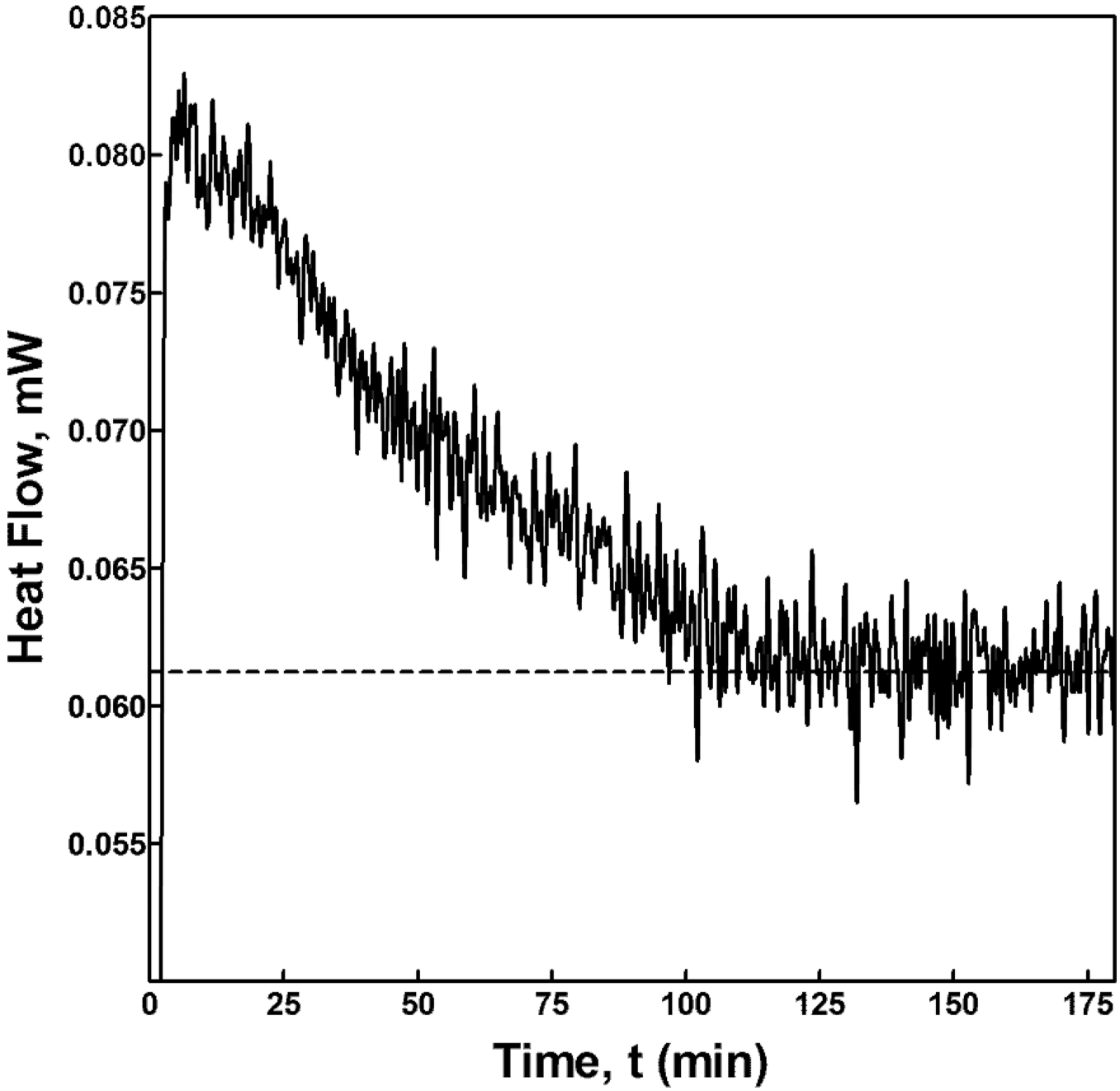

Figure 8.
DSC thermogram monitoring heat flow over time during the epoxy crosslinking reaction of a 10 wt% TGM and 7 wt% PAMAM solution in pH 7.4 PBS.

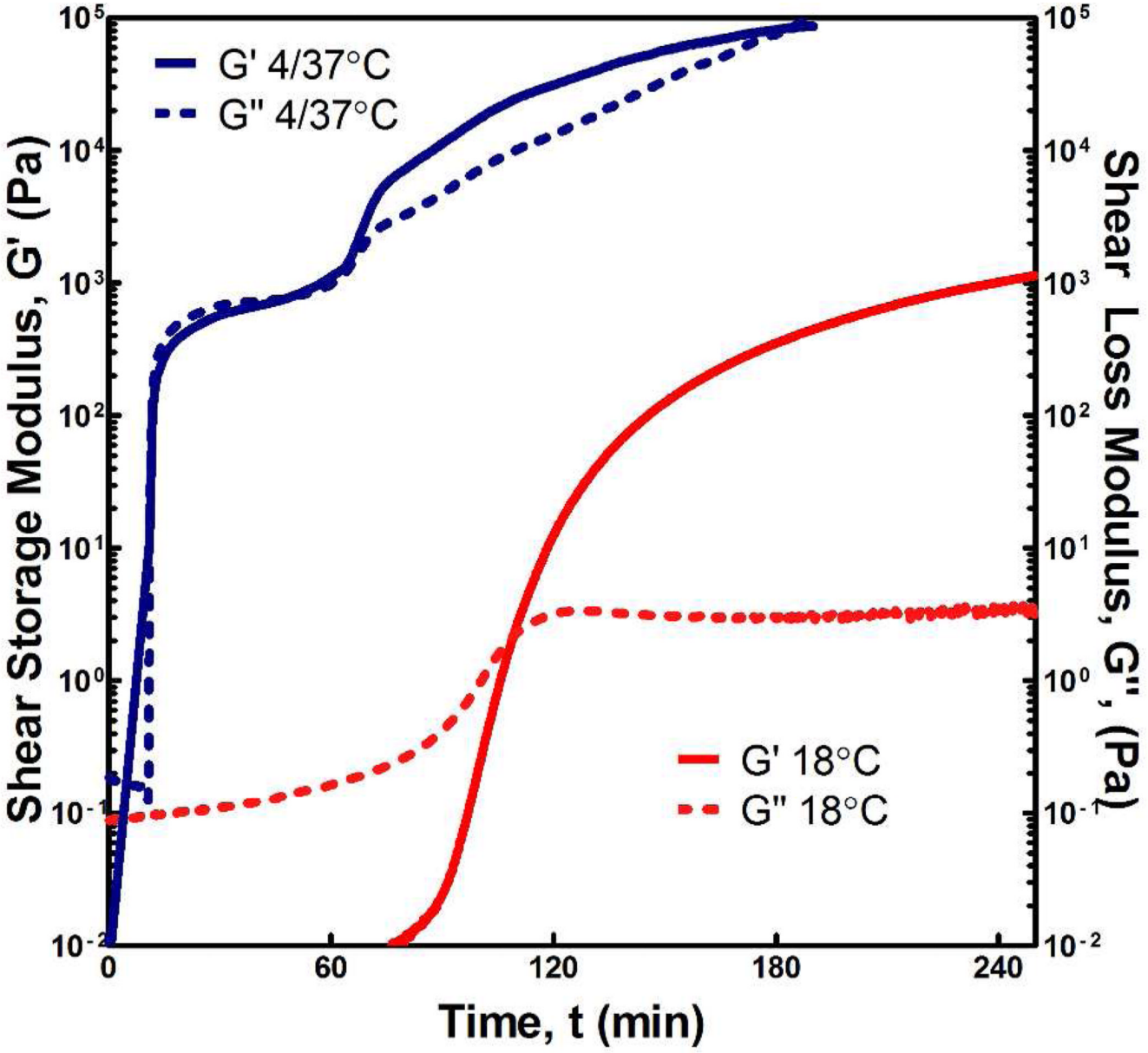

Figure 9.
Oscillatory rheology traces showing shear storage, G', and loss, G", moduli for an injectable hydrogel solution with 7 wt% PAMAM and 10 wt% TGM in pH 7.4 PBS either held at 18°C for 4 h or held first at 4°C for 10 min and then at 37°C for 3 h.

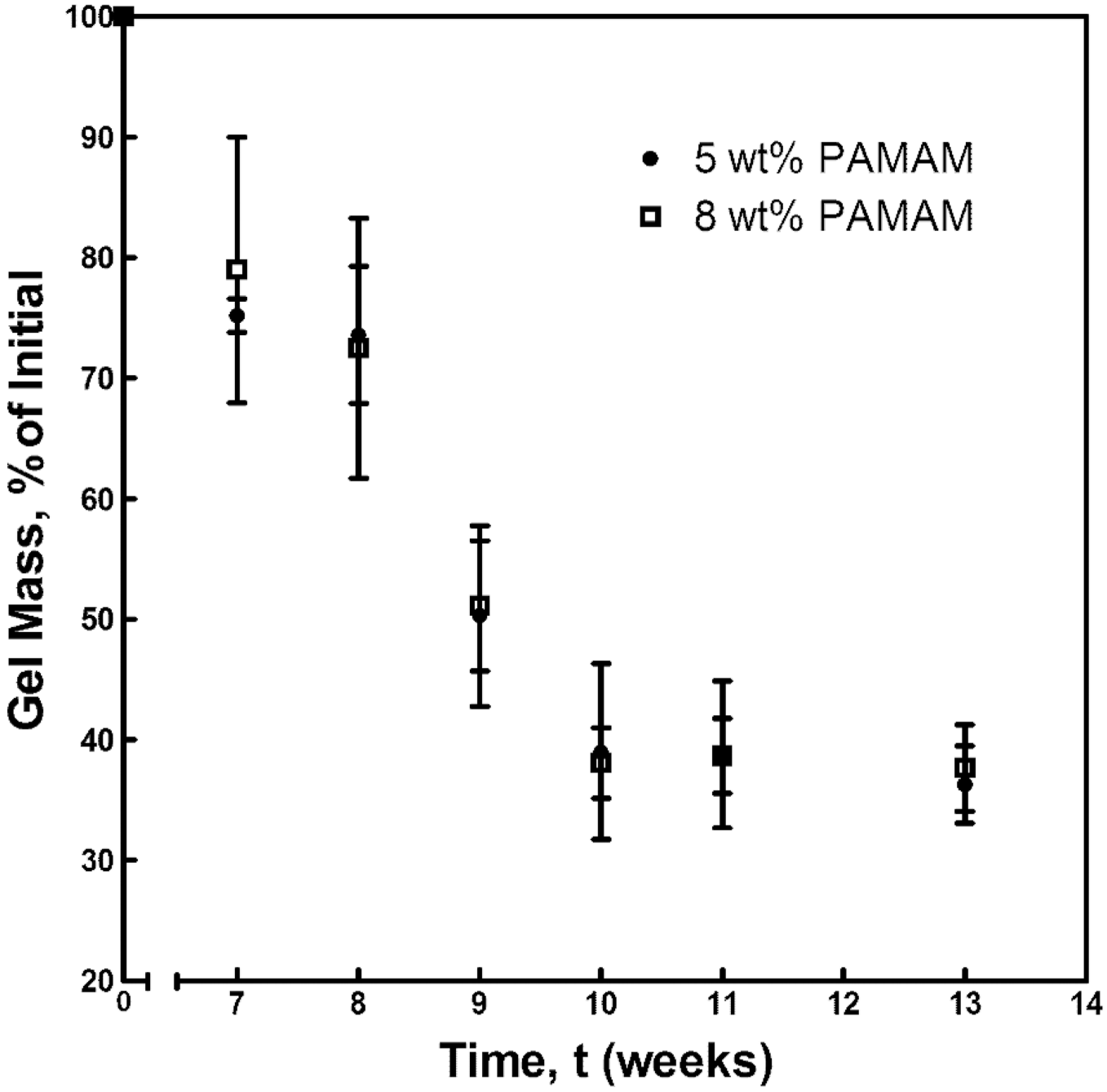

Figure 10.
Long-term mass loss due to PAMAM degradation in pH 7.4 PBS of hydrogels with 10 wt% TGM and either 5 or 8 wt% PAMAM.

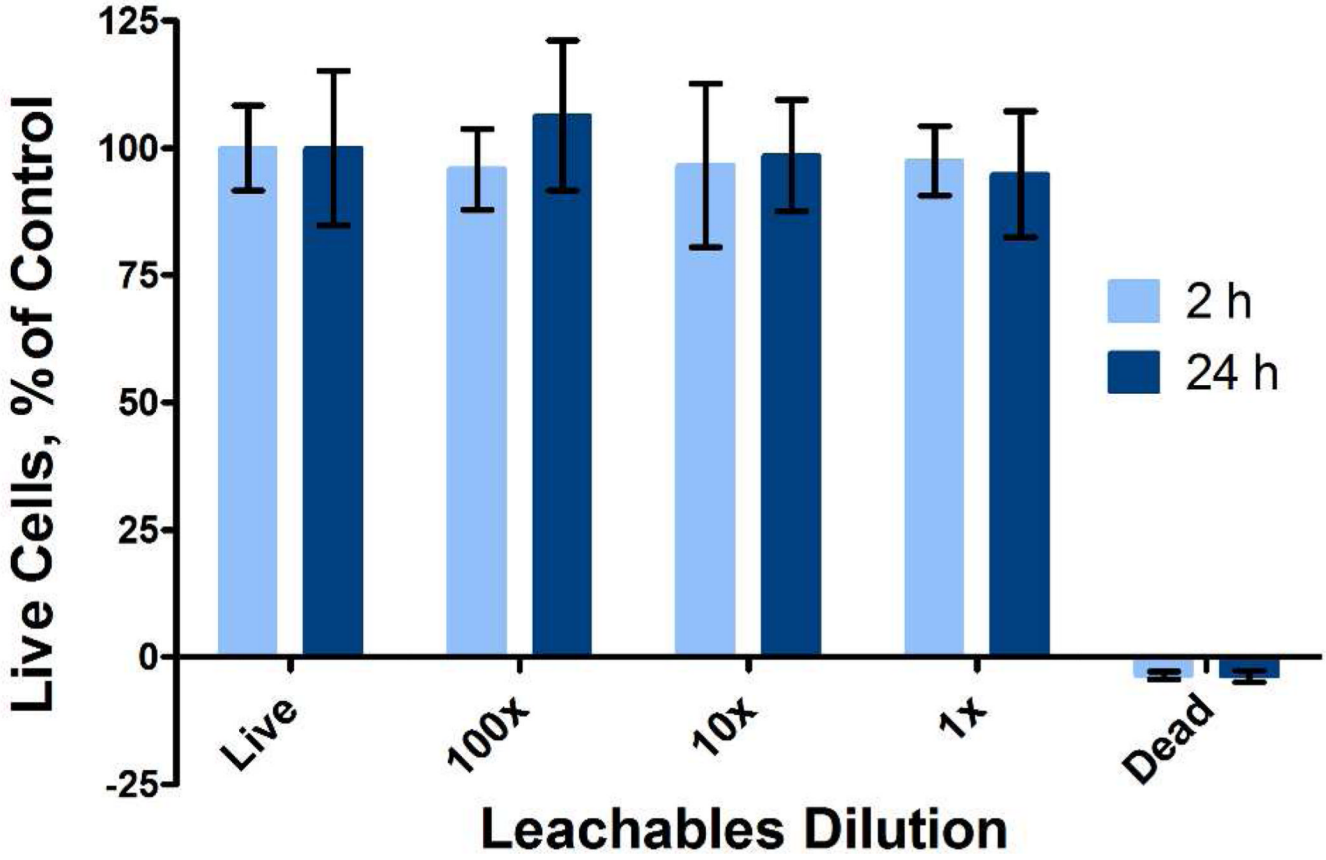

Figure 11.
Viability of rat fibroblasts exposed to soluble leachables from hydrogels with 7 wt% PAMAM and 10 wt% TGM in 1, 10, and 100x dilutions over 2 and 24 h relative to the live control as determined by fluorescence intensity from Live/Dead staining with live and dead controls shown.

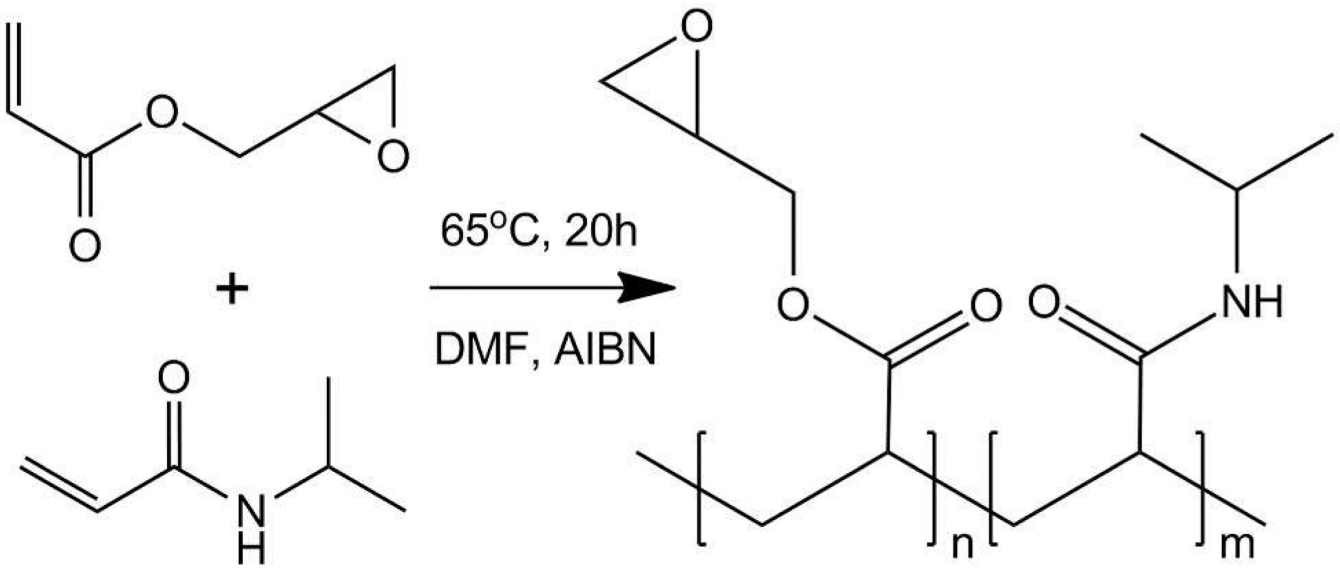

Scheme 1.
Synthesis of p(NiPAAm-co-GMA).

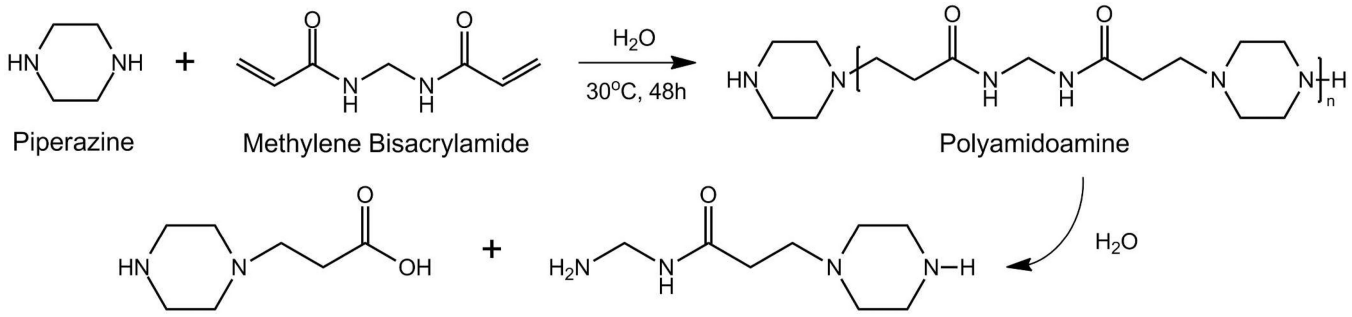

Scheme 2.

Synthesis and hydrolytic degradation of a polyamidoamine diamine macromer formed by polyaddition of piperazine and N,N'-methylenebisacrylamide.

Table 1

Molecular structure of primary, degradation, and secondary products of the PAMAM synthesis, as determined by microTOF mass spectroscopy, and their mol% of the total species present.

Structure	Mol %
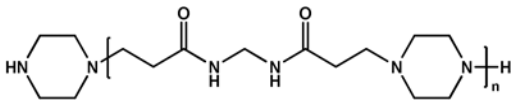	(a) 88.5
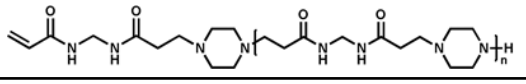	(b) 3.7
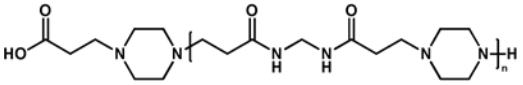	(c) 2.7
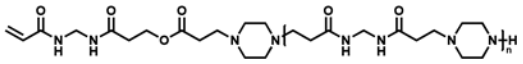	(d) 0.5
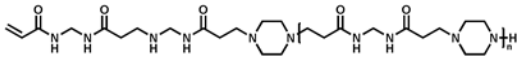	(e) 1.3
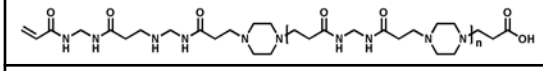	(f) 1.4
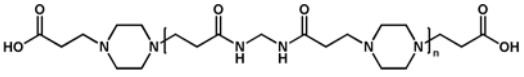	(g) 1.6
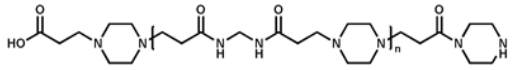	(h) 0.2

Table 2

PAMAM synthesis product distribution (mol% and wt%).

Synthesis Product	Mol %	Wt %
Desired Diamine	88.5%	95.2%
Heteroend Product	3.7%	1.3%
Degradation Products	7.8%	3.5%
• Mono-amine	4.7%	2.0%
• Other	3.1%	1.5%